# Virtual Time and Execution of Algorithms in Static Networks

**Dr Björn Graßl**[1]

[1]independent researcher, bjoern.grassl@gmx.de, https://orcid.org/0009-0005-8448-9855

## Abstract

A concept for the emergence of a time-equivalent property from a static network of interconnected states is shown. This property is referred to as virtual time. For each state, a set of coefficients is defined, which locally represents the information embedded in the network's connectivity. Network structures denoted as repellers feature successive splits into a steadily increasing number of quantum states. They convey an equivalent calculation of their static connectivity coefficients and virtual particles dynamically propagating within them. Strong indications are provided, that static networks are virtual Turing complete machines for algorithms with finite runtime. This opens up a wide range of possible encodings for said coefficients and motivates further research.

## Table of Contents

# 1 Introduction

Both the Standard Model and General Relativity consider spacetime [1] to be a fundamental entity. The idea of an emergent spacetime [2] became known primarily by Loop Quantum Gravity theories. The suggested mechanisms are sophisticated but complex, also because the complete 4-dimensional manifold together with spacetime metric is expected to emerge as a unit [3]. The emergence of an isolated virtual time in an initial step conceptually seems unattractive at first glance, as it additionally requires a mechanism for the generation of the time and space components of spacetime with the observable Minkowski metric in a successive step. However, this work shows a simple concept for this initial step, i.e. how an isolated time-equivalent property can be defined in a static network and how networks are able to execute algorithms with respect to this virtual time.

# 2 Motivation

Irrespective of potential further physical implications, the formalisms and methods presented in this work are interesting from a pure epistemological point of view alone. The following chapters will define “virtual time” as well as “network connectivity coefficients” and analyze the resulting logical conclusions. Although the concepts presented in this article do not directly lead to a fully-fledged theory for the emergence of spacetime, they open up new possibilities for hypothetical interactions between said algorithms, the different components of spacetime, gravity and the Standard Model.

Chapter 3.3 demonstrates, that the algorithms being virtually executed in static networks are conceptually able to represent physical processes of arbitrary complexity. In this context, it is beneficial to draw on existing formalisms from the field of computer science. Readers not interested in the proof of functional completeness might want to skip this chapter.

The exemplary model presented in the following chapter 2.1 is purely motivational and not necessary for understanding the actual methods and formalism. It should be considered as only one example that generally shows the versatile possibilities and motivates further research in this area. Due to the speculative character of the underlying idea, readers attaching particular importance to scientific rigor are advised to skip chapter 2.1 and continue reading directly with “Concepts and Methods” (chapter 3).

## *2.1 Speculative Extension of the Standard Model*

The beforementioned hypothetical interactions could for instance arise, if it is possible to extend the Standard Model to an effective quantum field theory [4] containing spacetime generating “particles”, which are coupling to conventional particles. As the following chapters demonstrate, in terms of virtual time static networks are able to execute algorithms. These algorithms can be designed to be equivalent to classical quantum mechanical particle generators. The algorithm presented in chapter 3.2.4.3 can be used to define the network connectivity coefficients of a state in the network in a way which corresponds to virtual particles arriving periodically in virtual time.

Speculatively, the observable time component of spacetime is the result of these particles, denoted as “time generating particles” (TGPs). It should be noted at this point, that TGPs refer to the observable time component of spacetime and therefore must not be confused with “virtual time” (see chapter 3.1.4), which is the basic property of the network enabling the execution of algorithms.

The energy contained in the TGPs could then be split to generate other particles in subsequent steps. These secondary particles could be responsible for the emergence of the spatial components of spacetime. Particles performing Lorentz boosts (LBPs) could prove to be particularly promising candidates for these “space generating particles”. Even though this concept is highly speculative, the extension of the Standard Model with TGPs and LBPs would feature some interesting characteristics:

1. Vacuum expansion could be identified as a process, when periodically arriving TGPs split their energy into LBPs. In the case of vacuum expansion, the LBPs do not interact with classical particles.
2. Since TGPs and LBPs contain energy, spacetime itself has to store this energy. This necessary requirement of the model is consistent with the observation of spontaneous particle antiparticle generation in pure vacuum.
3. Currently, "dark energy" is required to describe several cosmological observations, such as the rotation speed within galaxies. The energy contained in "spacetime generating particles" might be a potential new candidate for this dark energy.
4. As in case of all classical processes described by the Standard Model, also the total energy during interactions between TGPs, LBPs and classical particles has to be conserved. If the energy for generating classical particles or Lorentz boosting classical particles either exclusively or partially originates from TGPs or LBPs, the expansion of spacetime is expected to be reduced in comparison to the vacuum in the local proximity of interaction in spacetime. In its current stage, the model is too simple to predict the quantitative amount of reduction. However, the observed relativistic increase of spacetime curvature near massive objects qualitatively is consistent with the model.

# 3 Concepts and methods

## *3.1 Networks of interconnected States*

First, a concept is required, how a time-equivalent property can be emergent from a timeless, static network of interconnected quantum states. Conventionally, network interconnections represent quantum transitions. In this classical view, quantum states are changed at a specific time and in a specific sequence by a set of quantum operators complying to some quantum rules. However, in a static network a "chronological sequence" is intrinsically impossible.

### 3.1.1 Requirements

1. $V$ is a static network consisting of a finite number $n \in \mathbb{N}$ of quantum states.
2. A quantum parameter defines, whether quantum states are adjacent to each other or not.

For the purpose of clear presentation, the $n$ quantum states of the network are depicted as points. Lines represent adjacent quantum states. The result is a completely static representation of interconnected quantum states, independent from time. It is necessary to avoid thinking about trajectories, movements, or any temporal change of quantum states.

### 3.1.2 n-Neighborhood $N_n$

For a set of states $Q$ in $V$, the neighborhood $N_n$ ($n \in \mathbb{N}_0$) of $Q$ is defined as:

$n = 0$: $N_0(Q) = Q$

$n = 1$: $N_1(Q) = \{|b\rangle \mid |b\rangle$ is adjacent to any element in $Q\}$

$n > 1$: $N_n(Q) = N_1(N_{n-1}(Q))$

The case $n \geq 1$ represents the set of endpoints of all paths of interconnected quantum states with a length $n$ relative to any member of $Q$.

### 3.1.3 Metric *M*

Let $M(|a\rangle, |b\rangle)$ be a metric between $|a\rangle$ and $|b\rangle$ defined by:

$M: V \times V \rightarrow \mathbb{N}_0\,,\ M(|a\rangle, |b\rangle) \mapsto k$

$|a\rangle = |b\rangle$: $k = 0$

$|a\rangle \neq |b\rangle$: $k$ meets condition $|b\rangle \in N_k(|a\rangle) \wedge \overline{(\,|b\rangle \in N_l(|a\rangle))}\ \ \forall\, l \in \mathbb{N}_0 < k \in \mathbb{N}_0$

Thus, $M$ depicts the "shortest quantum distance" between $|a\rangle$ and $|b\rangle$ in terms of adjacency.

### 3.1.4 Virtual Time

#### *3.1.4.1 Model 1 with time*

The following first model represents the classical dynamic view. In this model, a chronological sequence of quantum transitions is investigated on a Planck scale ($t_0 \rightarrow t_0 + t_p \rightarrow t_0 + 2t_p$ ...). In this context, $\tilde{T}(|q\rangle)$ is defined as the set of all destination states of allowed quantum transitions from a source state $|q\rangle$. In this dynamic model, a valid quantum path $p$ with $n-1$ transitions from $|q_1\rangle$ to $|q_n\rangle$ is defined as:

**Eq 1:** $p = (|q_1\rangle, |q_2\rangle, \dots, |q_n\rangle\,) \ \mid\ |q_{i+1}\rangle \in \tilde{T}(|q_i\rangle)\ \forall\, 1 \leq i \leq n-1$

Each valid quantum path $p$ is defined to be consistent with the laws of nature. For sufficiently complex multi-particle states (e.g. if $|q_i\rangle$ represent states of the observable universe) and a sufficiently long pathlength, the laws of nature are embedded in the set $\{p\}$ of all valid paths.

#### *3.1.4.2 Model 2 without time*

In the second, static model, $n$-tuples of elements ($n \epsilon \mathbb{N}$) are defined, such that the elements of the tuple at adjacent indices contain adjacent (see requirement 2) states in $V$:

| | | |
|---|---|---|
| $p = (\lvert q_1\rangle)$ | | for $n = 1$ |
| $p = (\lvert q_1\rangle, \lvert q_2\rangle)$ | $\mid\ \lvert q_1\rangle \in N_1(\lvert q_2\rangle) \wedge \lvert q_2\rangle \in N_1(\lvert q_1\rangle)$ | for $n = 2$ |
| $p = (\lvert q_1\rangle, \lvert q_2\rangle, \dots, \lvert q_n\rangle\,)$ | $\mid\ \lvert q_{i\pm1}\rangle \in N_1(\lvert q_i\rangle)\ \forall\, 2 \leq i \leq n-1$ | for $n \geq 3$ |

Since $|a\rangle \in N_1(|b\rangle) \Leftrightarrow |b\rangle \in N_1(|a\rangle)$ this can be simplified as:

**Eq 2:** $p = (|q_1\rangle, |q_2\rangle, \dots, |q_n\rangle\,) \ \mid\ |q_{i+1}\rangle \in N_1(|q_i\rangle)\ \forall\, 1 \leq i \leq n-1$

This model only requires a mathematical order relation defined on the index number, but no progression of time.

**The definitions in the dynamic view (Eq 1) and the static view (Eq 2) are equivalent.**

Due to this equivalence, the static model is an alternative representation of the exact same physical processes taking place in the dynamic model. The effect of classical time is substituted by a property of the static network referred to as "virtual time". This property is exclusively defined by the network's connectivity. It is noteworthy, that virtual time is a local property of the network, as it depends on a reference state $|q\rangle$.

## 3.1.5 Network Connectivity Coefficients

### *3.1.5.1 Motivation*

If a quantum state is part of its own $m$-neighborhood $(\exists\, m \in \mathbb{N}_0 |\, |q\rangle \in N_m(|q\rangle))$ , its "functional role" in the network is defined by this specific $m$-neighborhood to a certain extent. Each quantum state within the network can be described by its connectivity with other states.

The equivalent phenomenon can also be seen in the dynamic view. Network loops represent a sequence of quantum transitions, where an initial quantum state is mapped onto itself. This suggests to analyze the ratio of feedback loops originating from each network state $|q\rangle$ for all possible quantum paths up to a specific length $n$ to investigate virtual temporal processes up to epoch $\tau = \mathrm{n}$. Let $p_i \in N_i(|q\rangle),\ i \in \mathbb{N}_0 \leq n$ the set of different quantum paths starting at $|q\rangle$ with $i$ quantum transitions and let $q_i$ the subset of $p_i$ of all feedback paths also ending in $|q\rangle$.

### *3.1.5.2 Definition*

This leads to $n$ coefficients for each $|q\rangle \epsilon V$:

Eq 3: $|q\rangle = \sum_{i=0}^{n} |q_i\rangle = \sum_{i=0}^{n} s_i\, |q\rangle$

$$\tilde{s}_i = \begin{cases} 1 \ \text{ for } i = 0 \\ \frac{|q_i|}{|p_i|} \ \text{ for } i > 0 \end{cases} \qquad \text{and normalized } s_i = \frac{\tilde{s}_i}{\sum_{i=0}^{n} \tilde{s}_i}$$

Figuratively speaking, the idea behind Eq 3 resembles the quantum mechanical concept of defining the identity operator via the spectral decomposition of a state.

### *3.1.5.3 Interpretation*

In the static view, each network state $|q\rangle$ is defined as a linear composition of itself using $n$ coefficients. These coefficients represent the influence of $|q\rangle$ on itself in terms of network loops up to length $n$.

However, in the dynamic view, a high value in $s_k(|q\rangle)$ means, that a significant part of energy of a virtual particle returns in $|q\rangle$ at epoch $k$, whereby the particle started its propagation through $V$ in $|q\rangle$ at epoch 0.

### *3.1.5.4 Normalizability*

In general, $n$ must be finite to ensure that $\sum_{i=0}^{n} \tilde{s}_i$ does not diverge. Divergence otherwise occurs for example in the connection layer states of oscillators (see below). As a counterexample, the coefficients of states within an infinite homogenous repeller (see below) can be normalized. Though normalizability seems desirable from a mathematical point of view, even a finite set of $n$ coefficients contains the complete information required to investigate virtual dynamic processes up to epoch $n$.

As the number of states in $V$ is finite (see "requirement 1"), the number of elements of the power set is finite. Then there exists a "most distant" $n_{max}$-neighborhood: $\forall k > n_{max}\ \exists i \leq n_{max} | N_i = N_k$ with $k, n_{max}, i \in \mathbb{N}_0$. Thus, the final state of every quantum path of arbitrary length must be an element of a finite set of neighborhoods. This realization motivates the conjecture, that the physical information encoded in the $s_i$ might be redundant for huge values of $n$, though the coefficients themselves not necessarily have to repeat.

Annotation: The above definition of the coefficients $s_i$ is particularly suited for establishing a direct equivalence between a static and a dynamic model. Therefore, it is used as the basis for this article. However, other coefficients expressing similar information about local network connectivity are also conceivable. An example is the always finite set of normalized coefficients $\hat{s}_i$, which indicate where $|q\rangle$ is part of its own $i$-neighborhood:

Eq 4: $$|q\rangle = \sum_{i=0}^{n_{max}} \hat{s}_i\, |q\rangle \text{ with } \hat{s}_i = \frac{\tilde{s}_i}{\sum_{i=0}^{n_{max}} \tilde{s}_i},\ \tilde{s}_i = \frac{\tilde{\theta}(|q\rangle, i)}{|N_i(|q\rangle)|},\ \tilde{\theta}(|q\rangle, i) = \begin{cases} 1 & \text{for } |q\rangle \in N_i(|q\rangle) \\ 0 & \text{otherwise} \end{cases}$$

Figuratively speaking, the coefficients $\hat{s}_i$ (Eq 4) count the destination state only once, whereas the coefficients $s_i$ (Eq 3) take each path to it into account.

## *3.2 Repellers*

Based on metric $M$, a state $|q\rangle \epsilon V$ can be located in an area of the network, which is hereby defined as a "repeller of length $m$ with regard to $|q\rangle$". The value of $m$ depicts the repeller's area of influence.

Equation 2 of the static model defines tuples $p$ of length $n$, such that the elements of the tuple at adjacent indices contain adjacent states in $V$. Let $P_n = \{p \mid |p| = n\}$ ($n \epsilon \mathbb{N}$) the set of all these $n$-tuples and let $\widetilde{M}_n$ be the expectation value of metric $M(p_1, p_n)$ for the corresponding first and the last element within each tuple in $P_n$.

### 3.2.1 Definition

State $|q\rangle$ is located inside a repeller of length $m$, if $\widetilde{M}_k$ increases strict monotonically with the length of the tuple: $\widetilde{M}_k \leq \widetilde{M}_{k+1} \forall 1 \leq k \leq m$

Fig 1 shows examples for states in a repeller of length 1 (A), of length 3 (B) and a counterexample (C).

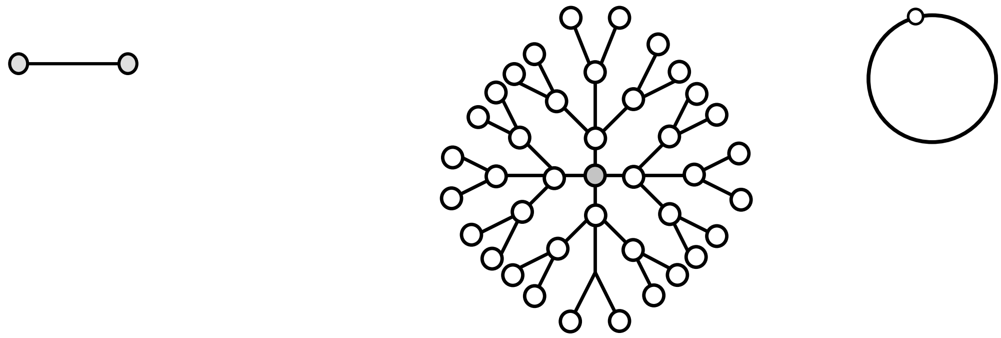

**Fig 1: Networks with and without repellers**

**(A)** The two states are located in a repeller of length 1 each.

**(B)** The state in the midpoint is located in a repeller of length 3.

**(C)** The state is not located in a repeller.

Within repellers, the mean quantum distance between $|q_1\rangle$ and $|q_i\rangle$ increases with the pathlength. Though repellers are defined as static structures, in the dynamic picture virtual particles propagate though the network under their influence. Figuratively speaking, the shortest way back (defined by metric $M$) for a particle to its source state gets longer and longer while propagating within a repeller.

### 3.2.2 Homogenous n-Repeller

Homogenous repellers are especially interesting, as they maintain constant growth of the distance $\widetilde{\mathrm{M}}_{k+1} - \widetilde{\mathrm{M}}_k$ with increasing $k$. The homogenous $n$-repeller is defined as a layered network structure, where one state of each layer is connected to $n$ states of the next layer. The network topology is independent of the position of states in the drawing (see Fig 2(A) and 2(B)).

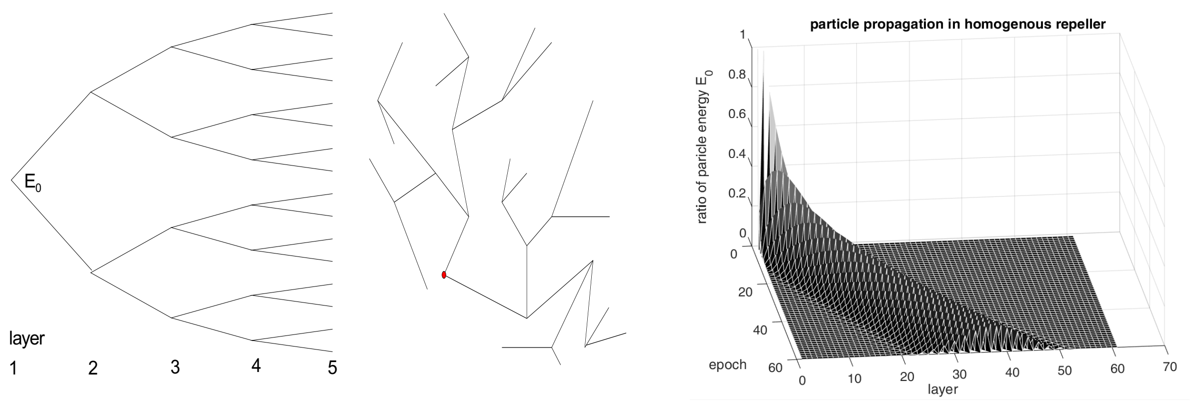


**Fig 2: The homogenous $n$-repeller**

**(A)** Homogenous 2-repeller, canonical representation, 5 layers. Metric $M$ increases with each layer from left to right.

**(B)** The same homogenous 2-repeller shown in (A) in distorted representation, 5 layers

**(C)** Simulation of virtual particle propagation in a homogenous 4-repeller over 60 epochs.
The group speed is constant.

Fig 2(C) visualizes the propagation of the energy of a virtual particle exemplarily starting from the single “top” state in a homogenous 4-repeller. For each new epoch, the energy in each state of the network is distributed equally to all neighboring states. The energy of the state at epoch 0 is designated as $E_0$.

- Epoch 0: $E_0$ is completely localized in layer 1 (single state)
- Epoch 1: $E_0$ is completely in layer 2 (distributed in the four states of layer 2)
- Epoch 2: $\frac{1}{5}E_0$ in layer 1, $\frac{4}{5}E_0$ in layer 3
- Epoch 3: $\frac{9}{25}E_0$ in layer 2, $\frac{16}{25}E_0$ in layer 4, …

Calculating the “repulsiveness” $R_k := \widetilde{\mathrm{M}}_{k+1} - \widetilde{\mathrm{M}}_k$ of $|q\rangle$ only makes sense if a general repeller does not decay into macroscopically distinguishable separate networks in terms of the metric $M$. Nevertheless, the repulsiveness is a meaningful value for homogeneous repellers and network structures which can be locally approximated by them.

Basic properties of homogenous $n$-repellers

- They require an exponential increase of quantum states to maintain their effect over increasing network distance (see Fig 2(A)).
- They feature a separation into an odd and an even neighborhood (see oscillation in Fig 2(C)):

  $$N_{k*2}(|q\rangle) \cap N_{l*2+1}(|q\rangle) = \emptyset \quad \forall\ k,l \in \mathbb{N}_0 \wedge k*2 \leq n \wedge l*2+1 \leq n.$$

- The repulsiveness $R_k = R$ is approximately constant for $0 \leq k \leq n-1$ (see Fig 2(C))

These results suggest the speculative hypothesis that the described time-equivalent property might be useful to find a mechanism for the emergence of spacetime and that the repulsiveness of repellers is required to keep physical processes running.

### 3.2.3 Basic Notations

× single network state

• set of multiple network states

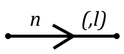


homogenous $n$-repeller of length $l$
the number of input and output states adjusts to the context and must be well defined. For example, the splitting ratio of the rightmost repeller in Fig 3 amounts to $n = 2^7$. This results directly from the connection diagram.

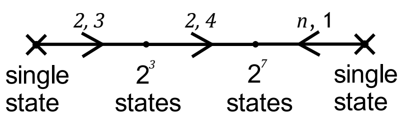

**Fig 3: Network with interconnected repellers. The splitting ratio $n = 2^7$ is defined by the connection diagram.**

The arrow notation of homogenous repellers can be used to define static networks very efficiently. Fig 4 shows the same network defined using the novel notation (Fig 4(A)) and completely displayed with all states and connection lines between adjacent states (Fig 4(B)). Due to the rapid increase of states in repellers from each layer to the next layer, more complex networks cannot be fully represented in practice.

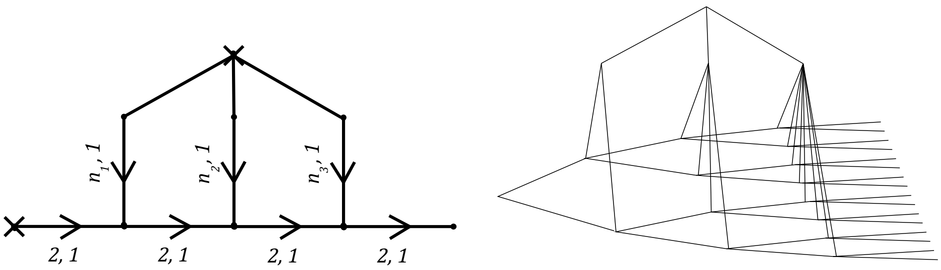


**Fig 4: Different representations of a simple static network**

**(A)** Static network defined using the arrow notation

**(B)** The same network displayed with all quantum states and interconnection lines

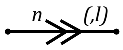

"strong" homogenous $n$-repeller, where $n$ is sufficiently huge, so that the energy diffusion of the virtual particle during $l$ epochs is negligible

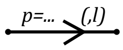

homogenous $n$-repeller of length $l$ with a transition probability $p$ from a network structure connected to its input into the repeller
$p = \frac{n}{n+k}$ , $k =$ number of network connections the repeller couples to

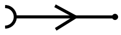
"signal follower", homogenous repeller with $p \approx 0$, so that the energy outflow from the network structure into the repeller is negligible.

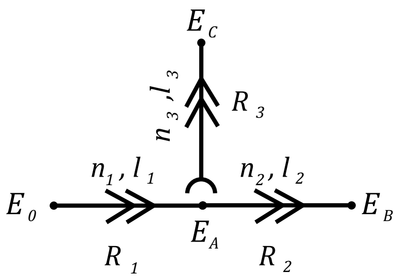


**Fig 5: Exemplary network with a signal follower**

The typical usage of a signal follower is depicted in Fig 5:

$E_0$ = energy of network at epoch 0
$E_A \approx E_0$ after $l_1$ epochs
$E_B \approx E_0$ after $l_1 + l_2$ epochs ($n_3$ must be sufficiently small)

$E_C \ll E_0$ after $l_1 + l_3$ epochs

Since in this example the signal follower is notated as a strong repeller, $n_3$ must additionally be sufficiently huge, so that energy diffusion within $R_3$ is negligible.

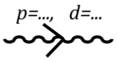


"field" of homogenous repellers coupling to a repeller $R$ with probability $p_F$ (field strength) and coupling density $d_F$ (field density of interaction). The model distinguishes between dense and strong fields. With $l$ = length of $R$, $k$ = number of coupling layers ($k \leq l$), and $d_F = \frac{k}{l}$ $(0 \leq d_F \leq 1)$, a "field" notates a series of $k$ repellers with coupling probability $p = p_F * d_F$, as can be seen in Fig 6.

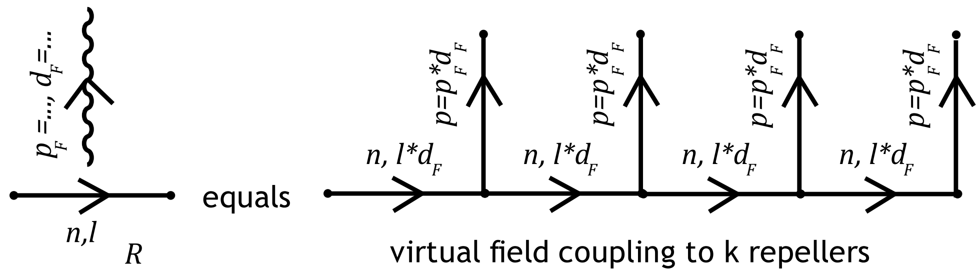


**Fig 6: virtual field consisting of *k* homogenous repellers**

## 3.2.4 Functions of Repellers

This paragraph demonstrates, how functional network units like oscillators, attenuators, delay units, logical gates, volatile and non-volatile memory can be realized based upon repellers. However, these units feature significant signal attenuation. Connected repellers are able to create network feedback loops and thus can exert influence on the coefficients $s_i$ of network states.

### *3.2.4.1 Delay unit, attenuation unit*

Repellers can be used to independently delay or attenuate signals. This is demonstrated by numerically simulating a virtual particle propagating through a network as depicted in Fig 7(A): The virtual particle with energy $E_0$ is propagating originating from layer 90 in $R_1$. In layer 100, the particle is split and $R_1$ couples to two repellers $R_2$ and $R_3$ with $p$=0.04. Afterwards, $R_3$ couples with $R_4$ in layer 106. There, $R_4$ acts as an attenuator and removes 50% of the energy from $R_3$.

The result can be seen in Fig 7(B): The split particles still feature equal energy in layer 102 ($E_{1,A}$ and $E_{2,A}$) after passing $R_2$ and $R_3$. When the particle from $R_2$ arrives at layer 120 ($E_{1,B}$), it features the regular amount of attenuation expected by its propagation within a "weak" repeller ($n = 40$). Although the particle from $R_3$ arrives at layer 120 in the same epoch, its signal ($E_{2,B}$) is attenuated by a factor of 2 in comparison to its counterpart from $R_2$.

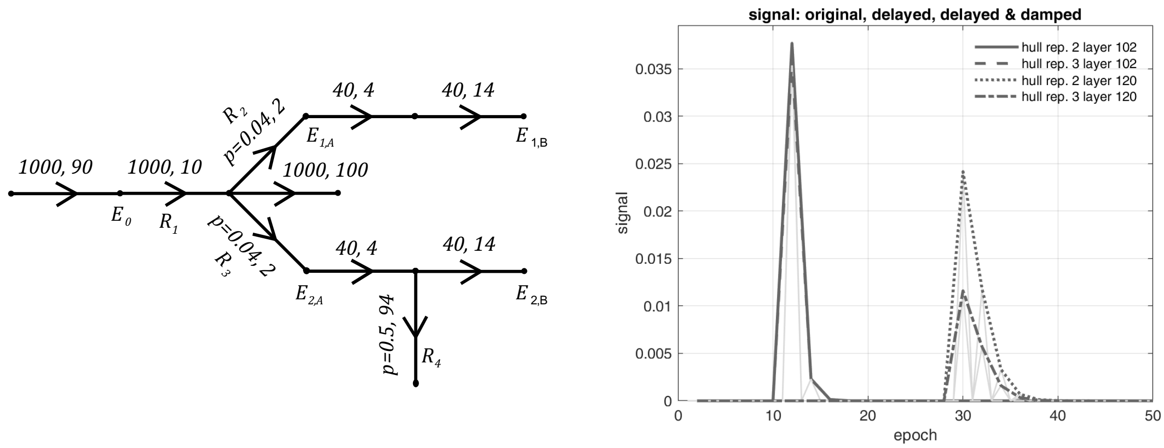


**Fig 7: Numerical simulation: delay and attenuation of repellers**

**(A)** Network schematics: A virtual particle propagates under the influence of repellers $R_{1\ldots4}$; Annotation: Since the simulation algorithm handles interactions sequentially ($R_1 \leftrightarrow R_2$ before $R_1 \leftrightarrow R_3$), $p_{sim,R3}$=0.0384 is slightly less than 0.04.

**(B)** Simulation result: The split parts of the particle arrive simultaneously at layer 120, but feature different attenuations: $E_{1,A}$ solid, $E_{2,A}$ dashed, $E_{1,B}$ dotted, $E_{2,B}$ dash-dotted

### *3.2.4.2 Oscillators*

If two repellers are connected in an opposing way, each state of the connection layer is associated with only one single state in each of the adjacent layers. This determines the behavior of the combined system, as can be seen in Fig 8(A).

If a virtual particle propagation contributes energy into this network structure, $R_1$ and $R_2$ function as a virtual oscillator in epoch τ as displayed in Fig 8(B):

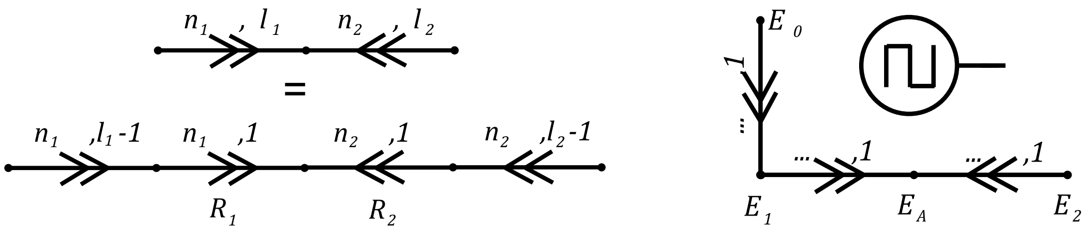


**Fig 8: Two strong repellers connected in "different directions" function as an oscillator**

**(A)** The upper network connection diagram can be reformulated in order to demonstrate that the oscillation only occurs in the innermost layer.

**(B)** Initial energy $E_0(\tau_0)$ is applied via the upper left repeller. This causes oscillation of $E_A(\tau)$

Let $\quad E_0(\tau_0) \neq 0,\ E_1(\tau_0) = E_A(\tau_0) = E_2(\tau_0) = 0$

then $E_A(\tau) = E_0 \wedge E_1(\tau) = E_2(\tau) = 0$ for $\tau - \tau_0$ even

and $E_A(\tau) = 0 \wedge E_1(\tau) = E_2(\tau) = \frac{E_0}{2}$ for $\tau - \tau_0$ odd and $\tau - \tau_0 \geq 3$

### *3.2.4.3 Generator of bit-pattern or waveform*

Network structures can be used to create every arbitrary finite energy amplitude in a state of the network as a function of virtual time. Therefore, a virtual particle propagation originating from a state $A$ with energy $E_0$ is equally split into $n_{max}$ separate branches. Each branch delays and attenuates its fraction of the original energy $E_0$ individually. The delay unit for $bit_k$ $(1 \leq k \leq n_{max})$ within the branches are homogenous repellers $R_k$ whose individual split ratios and lengths are calculated so, that after $k * L$ epochs ($L \in \mathbb{N}$) the initial fraction of $E_0$ fed into the repeller has diffused into the same number of states as in all other branches. Then, the states of the corresponding repeller's layer are interconnected to a single "energy collecting state" for each branch. To avoid oscillation, the rest of the energy is forwarded into a further repeller within each branch. Finally, the energy collecting states are recombined into state $B$. The bit-pattern generator can optionally be utilized as a waveform generator. In this case, the desired waveform is assembled by reducing the initial energy $E_0$ for each bit individually by a damping factor $\beta(W_{1\ldots n_{max}})$ mediated by the repellers $W_{1\ldots n_{max}}$.

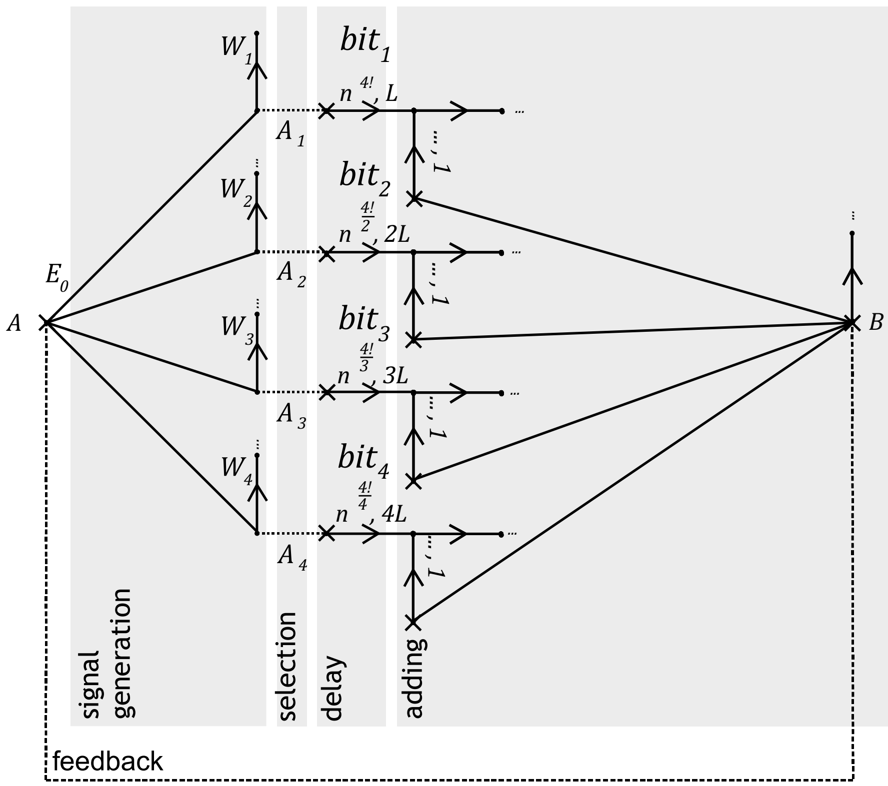


**Fig 9: Network connection diagram for the generation of custom bit-patterns and waveforms**

An example for four bits can be seen in Fig 9. $E_0$ in state $A$ is equally split into four branches. For each true bit, a corresponding delay repeller is connected to $A_{1\ldots4}$. The split ratio of this repeller is calculated individually for each bit so, that the corresponding interconnection layer of the three repellers consists of $n^{4!*L}$ states in each branch.

If for example all bits are true, a fraction of $E_0$ arrives after $k * L$ epochs in the corresponding interconnection layer. This fraction can be controlled by the splitting number of the "weighting repeller" $W_{1...4}$ for each bit. This also enables the generation of "analog waveforms". Some repellers in the following connection diagram are unnamed and followed up with three points. These repellers are used to avoid oscillations by forwarding the main amount of the propagating energy.

Optional feedback: The waveform generator can also be used to modify the coefficients $s_i$ in $A$ by connecting state $B$ back to state $A$ (dotted line in Fig 9).

The coefficients $s_i$ in state A for strong repellers, $k\epsilon\{1,2,3,4\}$, $L = 1$ and $\text{bit}_k\epsilon\{0,1\}$ are:

| **Index (epoch)** | 0 | 1..5 | 6 | 7 | 8 | 9 |
|---|---|---|---|---|---|---|
| **Value** | $s_0$ | *0* | $\alpha\ s_0\ \text{bit}_1\ \beta(W_1)$ | $\alpha\ s_0\ \text{bit}_2\ \beta(W_2)$ | $\alpha\ s_0\ \text{bit}_3\ \beta(W_3)$ | $\alpha\ s_0\ \text{bit}_4\ \beta(W_4)$ |

$\alpha$ is a constant factor depending on the initial value $s_0$, on the splitting number of the energy forwarding repellers and on the network structure they are connecting to. The damping factor $\beta(W_n)$ depends on the splitting number of repeller $W_n$.

## *3.3 Virtual Turing Completeness*

### 3.3.1 Requirements for logical operations

It is possible to perform calculations not only with the help of conventional electronic processors or digital circuits, but also using lesser-known units such as very energy efficient spin logic devices [5][6]. Logic calculations can also be carried out in a purely mechanical way, as in the case of the Zuse Z1 [7], based on an optical basis [8] or completely using analog circuits [9].

Among others things, logic values in static networks can be defined for example via the presence of oscillations with a specific frequency, significant patterns or amplitude modulations. The only goal of this chapter is to show that static networks feature similar properties as virtual Turing complete machines. The following concept of logic makes no claim to exclusivity. It is based on boolean logic and is not intended to be resource friendly in terms of required network size.

To provide a basis for boolean logical operations, a definition of what is logically true and false is required. For the following considerations, the truth values are defined relative to reference values. That means, a state $|q\rangle$ in the network is defined to be $|true\rangle$ in epoch τ, if its virtual energy is equal to a provided reference energy $|ref\rangle$: $E_{|q\rangle}(\tau) = E_{|ref\rangle}(\tau)$

Logical operations are performed by repellers, which involve delay and attenuation. Thus, the logical reference value in epoch $\tau$ must be retained for comparison to determine the truth value of the result. Since repellers can act as waveform generators, they are able to line up the logical result value with the reference value, where both are attenuated by the same factor. This can be used to directly control two consecutive self-influence coefficients $s_i$ and $s_{i+1}$ of a state in the network. Thus, in the dynamic view the result of a logical operation is defined to be $|true\rangle$, if the virtual energy in a state $|q\rangle$ of the network does not change its value during two consecutive epochs. Otherwise, it is defined to be $|false\rangle$.

### 3.3.2 XOR and AND

The network structure for the *XOR* gate is the attenuating adder (as already seen in the bit pattern generator from chapter 3.2.4.3). The *AND* gate uses the same structure, but attenuates the output by a factor of 2 more than the *XOR* gate.

With
$\left(E_{|false_{AND}\rangle} = 0.5\ E_{|ref\rangle} \vee E_{|false_{AND}\rangle} = 0\right) \wedge \left(E_{|false_{XOR}\rangle} = 2\ E_{|ref\rangle} \vee E_{|false_{XOR}\rangle} = 0\right)$

the absolute value differences of a $E_{|false\rangle}$ output from $E_{|ref\rangle}$ are
$d_{min} = \frac{E_{|ref\rangle}}{2}$ and $d_{max} = E_{|ref\rangle}$

### 3.3.3 Cascading gates

When sequentially stacking $n$ gates (*AND* or *XOR*), all outputs $E_{|out_i\rangle}$ for $1 \leq i \leq n$ are simply added. The cascaded output is $|true\rangle$, if and only if $\sum_{i=1}^{n} E_{|out_i\rangle} = \sum_{i=1}^{n} E_{|ref_i\rangle}$.

This requires, that the attenuation from each gate to the next gate fulfills the condition $\frac{E_{|\mathrm{ref}_{i-1}\rangle}}{E_{|\mathrm{ref}_i\rangle}} > 4$ for $2 \leq i \leq n$, because then $\sum_{k=i}^{n} d_{max_k} < d_{min_{i-1}}$. Figuratively speaking, the $|false\rangle$ output of a *XOR*($|true\rangle, |true\rangle$) gate cannot be compensated by any number of following $|false\rangle$ outputs of *AND*($|false\rangle, |false\rangle$) gates.

### 3.3.4 Functional Completeness

The logical operations *XOR* and *AND* with $|true\rangle$ are functionally complete, since all other basic logical operations can be derived from them as described by de Morgan's laws. In particular
*NOT*($|a\rangle$)=*XOR*($|a\rangle, |true\rangle$) and *OR*($|a\rangle, |b\rangle$)=*NOT*$\Big(AND\big(NOT(|a\rangle), NOT(|b\rangle)\big)\Big)$.

### 3.3.5 Conditional Branches and Memory

Functional completeness alone already enables complex calculations. However, the following concepts of conditional branching and memory demonstrate even increased flexibility while executing algorithms in static networks.

For algorithms with finite runtime, conditional branches can be realized by using two independent subnetworks, each of which represents one possible branch with all previously performed logic operations.

With regard to the defined logic, a virtual particle propagating within a strong homogenous repeller remains its logical value over many epochs. Thus, it is able to represent a non-volatile bit. In contrast to this, a volatile bit can be able to be cleared at certain epochs in a controlled manner. This can be achieved via a sparse repeller field (see chapter 3.2.3), which removes energy at specific layers. In that way, volatile bits have the property of being erasable and redefinable.

Functional completeness in combination with the realizability of memory and conditional branching suggests that static networks represent virtual isolated Turing machines [10] [11] which are able to execute non-interactive, deterministic programs restricted to finite runtime. Functional completeness has a great impact on how the coefficients $s_i$ might be able to encode a state $|q\rangle$ [12].

# 4 Results

A static model of network connectivity and a dynamic model of quantum transitions were provided. Their comparison revealed, that they feature equivalent definitions. This was used to define a time-equivalent property in static networks, which depends on individual states.

For each state a set of coefficients was defined, which figuratively speaking describe the network's influence of the state on itself. They are calculated directly from the connectivity of the network, without any necessity for time. Therefore, the relative ratio of feedback paths to all paths up to a specific length was calculated. Particularly significant here are network structures designated as "repellers", a network topology in which quantum paths originating in a state lead further away with increasing quantum pathlength in terms of the metric of shortest quantum distance. This is achieved by a successive split into a steadily increasing number of quantum states. A meaningful arrow notation was defined that makes it easy to handle the rapid network growth. Homogenous repellers convey an equivalency between their connectivity and virtual particles propagating within. Thus, they act as repulsive units in a time-equivalent image. By interconnecting repellers, more complex functional units are defined, which perform specific dynamic operations such as attenuation, delay, oscillation, logical functions. Functional Completeness was proved and strong indications were provided, that by combining these units, virtual Turing complete machines for any deterministic, non-interactive algorithm restricted to finite execution time can be represented by static networks.

# 5 Discussion

The novel concepts presented in this work might be interesting from a pure methodological point of view. However, the new approach might also provide insights for further physical research.

Previous results [13] suggest a new hypothetical concept of spacetime, where in non-relativistic approximation and Minkowski view [14] the complete information of spacetime can be reconstructed from a “here and now” state $|\mathrm{Y}_0\rangle$ by applying permutations of operators $\mathrm{LEFT}_n$ $\mathrm{TOP}_n$, $\mathrm{FRONT}_n$, $\mathrm{P}_n$ to $|\mathrm{Y}_0\rangle$. The new results motivate to speculate about whether the network connectivity coefficients $s_i$ might also be able to represent the same information and whether spacetime, the Standard Model and gravity could hypothetically be emergent from a static quantum network.

If at all possible, the reconstruction of spacetime, the understanding the encoding of the coefficients $s_i$, the generalization of $\mathrm{P}_n$, $\mathrm{LEFT}_n$ $\mathrm{TOP}_n$, $\mathrm{FRONT}_n$ to relativistic operators and the definition of their operator counterparts acting on states in the network *V* are not trivial. If this approach turns out to be effective, a lot of research will be needed before eventually obtaining a completely symmetric unification theory.

# 6 Declarations

## 6.1 *Funding*

The author declares that no financial support was received for the research, authorship, and/or publication of this article.

## 6.2 *Competing interests*

The author declares that the research was conducted in the absence of any commercial or financial relationships that could be construed as a potential conflict of interest.

## 6.3 *Data and Code availability*

No additional data was used for this article.

No additional code is required to reproduce the results of this article.

*For peer review, the code for generating Figure 3 can be downloaded from the Open Science Framework: https://osf.io/bj4s2/?view_only=bad62fd4a86442cbab59c1c70f5dea1f*

## 6.4 *Author contributions*

BG: Conceptualization, Methodology, Writing, Simulation

# Acknowledgments

I thank Dr Stefan Schuberth and Dr Jan Krauß for valuable discussions.

# 7 References

1. Wagner, S., Existence of Minkowski space, 2016, arXiv:1610.00992
2. Oriti, D., “Levels of spacetime emergence in quantum gravity”, 2018, arXiv:1807.04875v1
3. Ashtekar, A., A Short Review of Loop Quantum Gravity, 2021, arXiv:2104.04394
4. Carroll, S., The Quantum Field Theory on Which the Everyday World Supervenes, 2021, arXiv:2101.07884
5. Debashis, P., Chen, Z., Experimental Demonstration of a Spin Logic Device with Deterministic and Stochastic Mode of Operation., Sci Rep 8, 11405 (2018), doi:10.1038/s41598-018-29601-5
6. Agarwal, H., Pramanik, S., Bandyopadhyay, S., Single spin universal Boolean logic gate., 2008, New Journal of Physics - NEW J PHYS. 10. 10.1088/1367-2630/10/1/015001.
7. Rojas, R., Konrad Zuse's legacy: the architecture of the Z1 and Z3, IEEE Annals of the History of Computing, vol. 19, no. 2, pp. 5-16, April-June 1997, doi: 10.1109/85.586067
8. Tucker, R. S., The role of optics in computing., Nature Photonics. volume 4 number 7, 2010, page 405, doi:10.1038/nphoton.2010.162
9. Maxwell, C. G., Analog Computer Staff, Handbook of Analog Computation (Including Application of Digital Control Logic), 1967, Systron Donner Corporation, chapter 2,3
10. Turing, A. M., On Computable Numbers, with an Application to the Entscheidungsproblem., Proceedings of the London Mathematical Society, volume s2-42 issue 1, 1937, ISSN 0024-6115, pages 230–265, doi:10.1112/plms/s2-42.1.230
11. Turing at 100, Nature 482, 440 (2012). doi: 10.1038/482440a
12. Feynman, R. P., Simulating Physics with computers., 1982, International Journal of Theoretical Physics. Bd. 21, Nr. 6/7
13. Graßl, B., Hypothetical axiom of Complete Symmetry and a new concept of spacetime, 2025, Zenodo, doi: 10.5281/zenodo.14634536
14. Hwang, P. W., We live in the quantum 4-dimensional Minkowski space-time., 2015, arXiv:1506.08543